IECG 2020

sciforum

Conference Proceedings Paper

Refining IKONOS DEM for Dehradun Region using Photogrammetry based DEM Editing Methods, Orthoimage Generation and Quality Assessment of Cartosat-1 DEM

Ashutosh Bhardwaj [1]*, Kamal Jain [2] and R.S. Chatterjee [3]

Published: date
Academic Editor: name

[1] Indian Institute of Remote Sensing, Dehradun; ashutosh@iirs.gov.in
[2] Indian Institute of Technology, Roorkee; kamal.jain@ce.iitr.ac.in
[3] Indian Institute of Remote Sensing, Dehradun; rschatterjee@iirs.gov.in

* Correspondence: ashutosh@iirs.gov.in; Tel.: +91-941-031-9433

Abstract: The correct representation of the topography of terrain is an important requirement to generate photogrammetric products such as orthoimages and maps from high-resolution (HR) or very high resolution (VHR) satellite datasets. The refining of the digital elevation model (DEM) for the generation of orthoimage is a vital step with a direct effect on the final accuracy achieved in the orthoimages. The refined DEM has potential applications in various domains of Earth sciences such as geomorphological analysis, flood inundation mapping, hydrological analysis, large scale mapping in an urban environment, etc., impacting the resulting output accuracy. Manual editing is done in the presented study for the automatically generated DEM from IKONOS data consequent to the satellite triangulation with a root mean square error (RMSE) of 0.46, using the rational function model (RFM) and an optimal number of ground control points (GCPs). The RFM includes the rational polynomial coefficients (RPCs) to build the relation between image-space and ground-space. The automatically generated DEM initially represents the digital surface model (DSM) which is used to generate a digital terrain model (DTM) in this study for improving orthoimages for an area of approximately 100 km^2. DSM frequently has errors due to mass points in hanging (floating) or digging, which need correction while generating DTM. The DTM assists in the removal of the geometric effects (errors) of ground relief present in the DEM (i.e., DSM here) while generating the orthoimages and thus improves the quality of orthoimages, especially in areas like Dehradun which is having highly undulating terrain with a large number of natural drainages. The difference image of reference i.e. edited IKONOS DEM (now representing DTM) and automatically generated IKONOS DEM, i.e. DSM has a mean difference of 1.421 m. The difference DEM (dDEM) for the reference IKONOS DEM and generated Cartosat-1 DEM at 10m posting interval (referred to as Carto10 DEM), results in a mean difference of 8.74 m.

Keywords: Digital surface model, Digital terrain model, Difference DEM, Rational Function Model, Satellite Triangulation, Hanging (floating) mass points, digging mass points.

1. Introduction

Digital Elevation Model (DEM) is the digital geometrical representation of elevation at a place (terrain), either in raster or vector form with regular or irregularly distributed points. DEM is often used as a generic term for elevation at a pixel and can refer to DSM and DTM as per the context or application [1]–[4]. The editing of a digital elevation model is an important step in the production of an accurate topography for a region. Several automatic procedures have been developed over time, however, they are not able to match the manually corrected DEMs. The disadvantage of manual corrections on the other hand includes the requirement of the trained work-force, cost, and high-end photogrammetric systems besides time. However, for important tasks and study areas, still, the manual corrections are the best option for achieving an accurate topography using Photogrammetric techniques, which have the potential to affect the required application positively and improve results.

The application scientists and researchers have also explored the advantages with the improved DEMs for specific applications. Physically-based GIS models, such as Transient Rainfall Infiltration and Grid-based Regional Slope stability (TRIGRS), using pore pressure calculations, compute the transient degradation of the hillslope stability due to rainfall infiltration to identify the landslide occurrences in the Guwahati city. Significantly different outputs were obtained for the different DEMs tested in the experiment, highlighting the importance of the analysis with different datasets [5]. The study has shown that an increase of slope by 1 degree, the initial factor of safety (FOS) against landslide triggering is reduced by 2.32% for a given soil material. Soil properties and rainfall intensity were found to be the primary factors controlling the instability of slopes due to rainfall, while the initial water table (WT) location and slope geometry plays a secondary role [6]. The source of the datasets is an important consideration; and at times, the finer resolution may not necessarily result in higher predictive accuracy due to artifacts and can have a significant influence on the accuracy of a landslide susceptibility analysis as found in the study using the integration of AHP and likelihood ratio (hybrid L-AHP) [7].

Researchers have attempted improvements in DEM using DEM fusion approaches and achieved significant accuracies through it at various experimental sites [8]–[13]. DEM fusion is also used for the generation of improved DEM at a global scale for various applications such as hydrological and flood analysis [11], [12], [14]. DEMs are used for monitoring and measuring gully erosion in geomorphologically unstable environments. Gully degradation rates measured based on DEMs are directly proportional to the square root of the gully area [15]. The mean water surface elevations (WSE) along the stream and the flood inundation area for five streams show a strong positive linear relationship with DEM grid size under identical boundary conditions for all the sites [16]. Unmanned Aerial Vehicles (UAVs) and ground-based LiDAR solutions are used for DEM fusion using three methods available in the mosaic tool, ArcGIS (Cover method, Average method) and GRASS (MBlend method). Cellular Automata Dual-DraInagE Simulation (CADDIES) model is used for the assessment of urban floods by analysis of water depth and flow velocity to further estimate flood hazard along evacuation routes [17]. DEM and Orthoimage maps provide basic layers for many geographic information systems (GIS) based analysis [18]. The presented study showcases the DEM editing requirements for undulating terrain at Dehradun and improved representation of topography as a DTM for the experimental site. Also, the present study aims to demonstrate the problems and quality assessment of the automatically generated DEMs, which are DSMs generated as the primary product from the initial photogrammetric solutions.

2. Material and methods

2.1 Study area

The study area falls in the Dehradun district of Uttarakhand and covers a major part of Dehradun city as shown in Figure 1. The site is marked with undulating terrain and has a dense drainage network, which is mostly seasonal. The area receives an average annual rainfall of about 207.3 cm. Dehradun is the provisional capital city of the Uttarakhand state, India. It is located in the

Doon valley, 260 km north of India's capital New Delhi. The Dehradun site is characterized by highly rugged terrain comprising of Shivalik hills in the south and higher Himalayas on the north, the river Ganga in the east, and the river Yamuna in the west. In the south, it has plain agricultural fields. The forest area in the study site comprises of Sal (dry deciduous), and Sal mixed (dry deciduous). Forest density in Dehradun site may be classified into various categorized namely, very dense forest (canopy density > 70%), moderate dense forest (canopy density: 40% - 70%). Some areas are as open forest (canopy density: 10% - 40%) and scrub (canopy density: < 10%) [19].

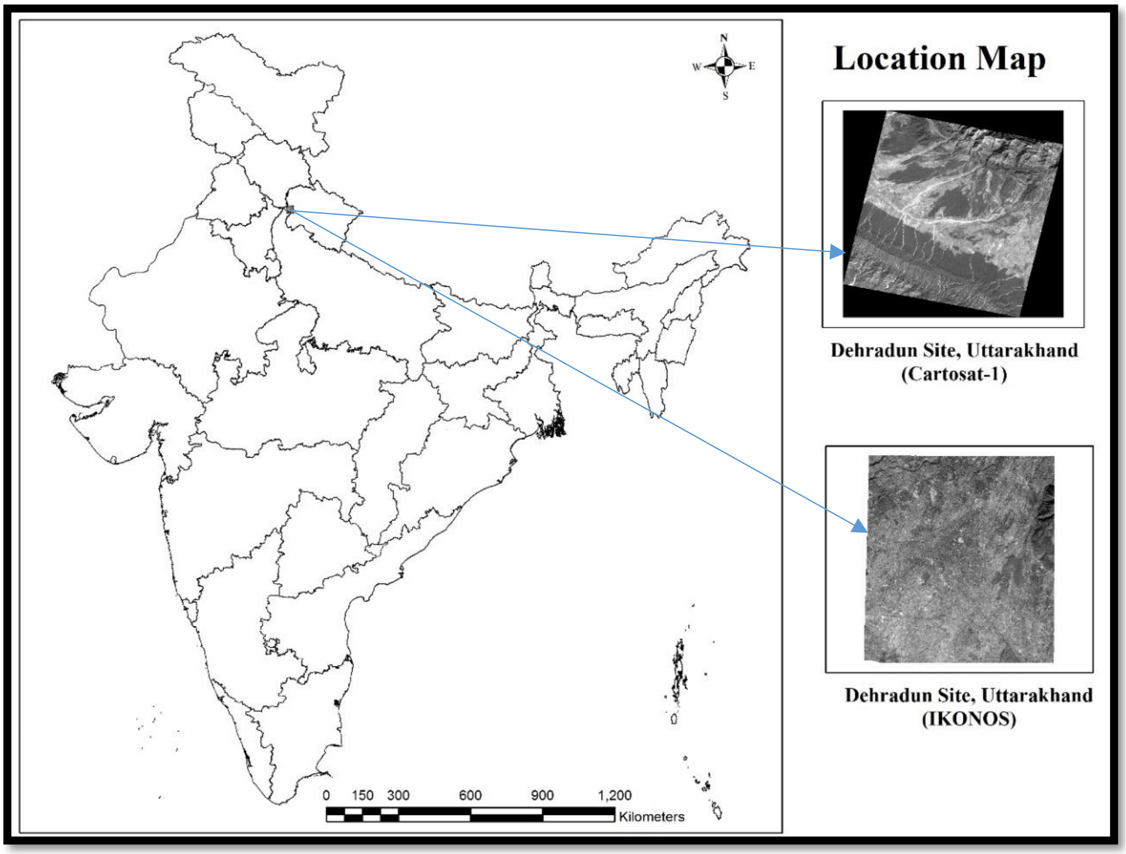

Figure 1. Location map of the experimental site

2.2 Data used

a) IKONOS-2 Geostereo

IKONOS-2 launched by the United States successfully on Sept. 24, 1999, was the first successful commercial remote sensing satellite which provided PAN stereo data with 1m spatial resolution and 4m multispectral data. The satellite was designed and built by Lockheed Martin Commercial Space Systems. The geometric models used for IKONOS basic imagery utilize the RFM having RPCs distributed by Space Imaging Company. The spacecraft provides precision pointing to an ultra-stable highly agile platform, giving it an excellent observation capability for the acquisition of VHR images (Table 1). IKONOS had 3800 pixels generating a swath width of 11.3 km in the case of a nadir view with original pixel size on the ground of a spatial resolution 82 cm [20], [21]. Figure 1 shows standard geometrically corrected Geo stereo product scenes of IKONOS-2 stereo pairs (one each) with respective image IDs. The area of interest (AOI) was covered in two IKONOS-2 stereopairs, so the area covered by Figure 2(a) and Figure 2(b) are covering different regions as per the AOI, with a total area of $100km^2$. $100km^2$ was also the minimum data order size required while procurement of IKONOS stereo data.

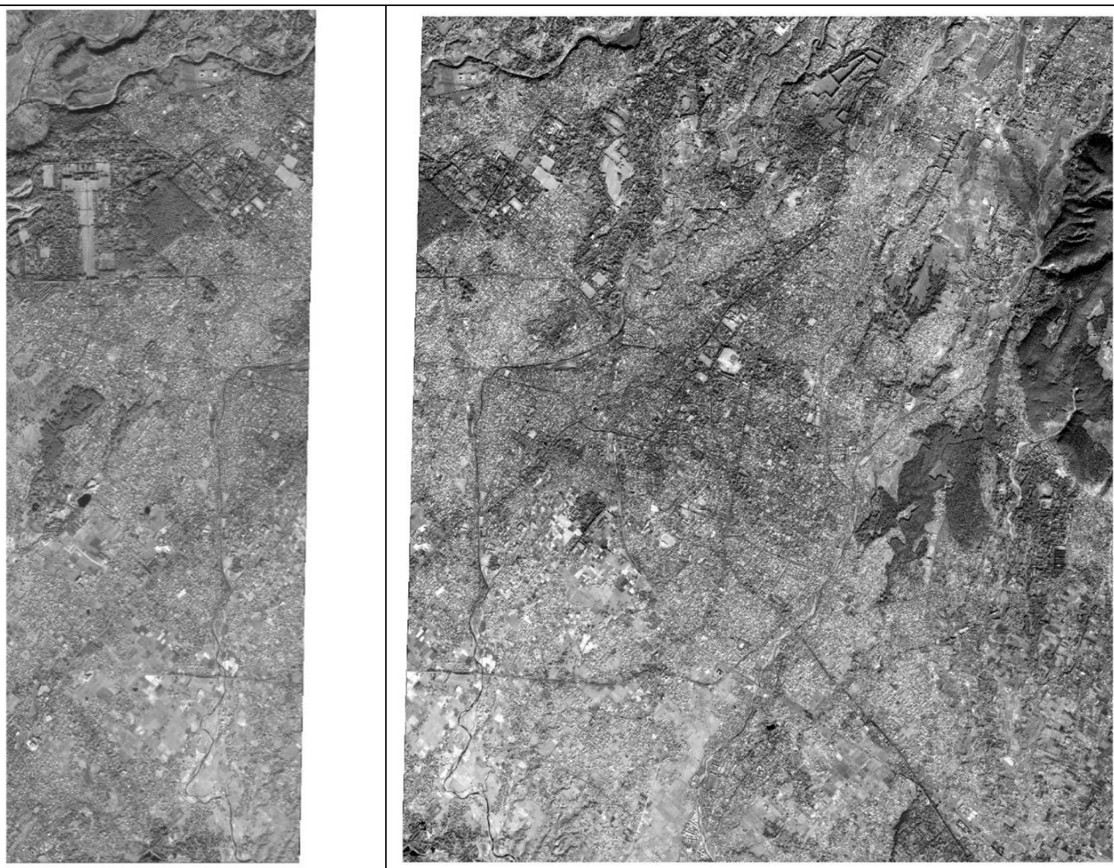

(**a**) (**b**)

Figure 2. IKONOS-2 Stereo pair images (one each): (a) Scene-1 (Source Image ID: 2010112605334560000011608311), (b) Scene-2 (Source Image ID: 2010112605331100000011608312)

Table 1. Specification of the IKONOS Satellite

Product	Specifications
Altitude	681 km
Orbit	Sun-synchronous orbit
Nodal crossing	10:30 am
Spectral Range	450-900 nm
Dynamic range	11 bits per pixel
Swath	11.3 km (at nadir)
Slew rate	10 seconds to slew 200 km
Data acquisition	51 x 112 km maximum mono collection per pass (5 strips) 11 x 120 km maximum stereo collection per pass (1 pair)
Datum	WGS84
Ellipsoid	WGS84

b) Cartosat-1 stereopair

Cartosat-1 launched on May 5, 2005, was the first Indian satellite capable of providing in-orbit along-track stereoscopic images and designed for applications, such as cartography, terrain modelling, natural resource management, and large-scale mapping. The Cartosat-1 image covering the Dehradun site is shown in Figure 3 and the specifications of Cartosat-1 are shown in Table 2.

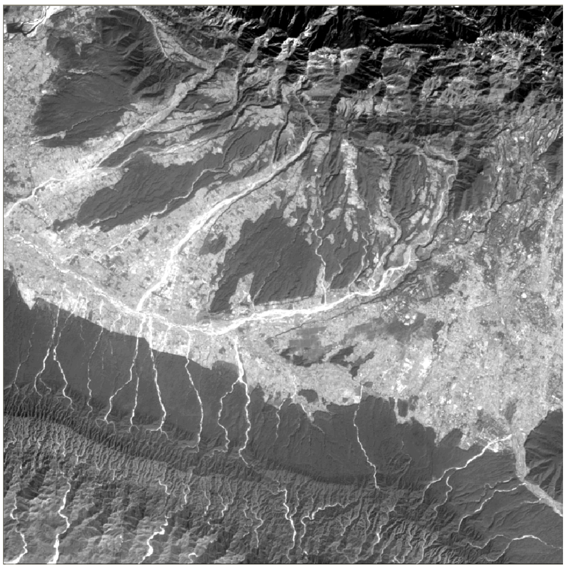

Figure 3. Cartosat-1 image for Dehradun site

Table 2. Specifications of CARTOSAT-1 satellite & Scene Description of stereo pair

Study area	**Dehradun site**	
Imaging mode	Stereo	Stereo
Processing Level	STD (Standard Geometrically Corrected)	
Product ID	065121300101	065121300102
Product Type	Orthokit	Orthokit
Image Format	GeoTIFF	GeoTIFF
Date of acquisition	05 Feb.2006	05 Feb.2006
Image Type(Sensor)	PAN	PAN
Time	05:34:44:1560	05:35:36:2857
Orbit Number	4091	4091
Stereo position	FORE	AFT
Path-Row	0526-0258	0526-0258
SceneCenterLat	30.35142241	30.35141408
SceneCenterLon	77.91655232	77.91245328
Swath	30km	
Dynamic Range	10 bits	
Ellipsoid	WGS84	
Datum	WGS84	
Interpolation Method	Cubic Convolution	

2.3 Toposheets

Survey of India (SOI) toposheets namely, 53F/15, 53F/16, 53J/3, and 53J/4 were used during the fieldwork and analysis during the study.

2.4 GPS data

Differential GPS data were collected through field surveys using Leica 500 series and Trimble R7 GNSS receivers.

3. Methodology

Satellite triangulation is done using five number (optimal) of GCPs providing control at the periphery (corners) and near the center of stereopair along with the RPCs resulting in a root mean square error (RMSE) of 0.46. The manual editing of DEM is performed in the interactive terrain editor (ITE) of Leica Photogrammetric Suite (LPS) software. The main steps are shown in Figure 4. Mainly three methods were used in ITE for DEM correction: a) Grabbing and placing the mass point at the correct place on the terrain; b) deletion of floating/digging mass points and placing the new mass points on the correct place over the terrain; and c) breaklines were added at locations of steep changes in elevations.

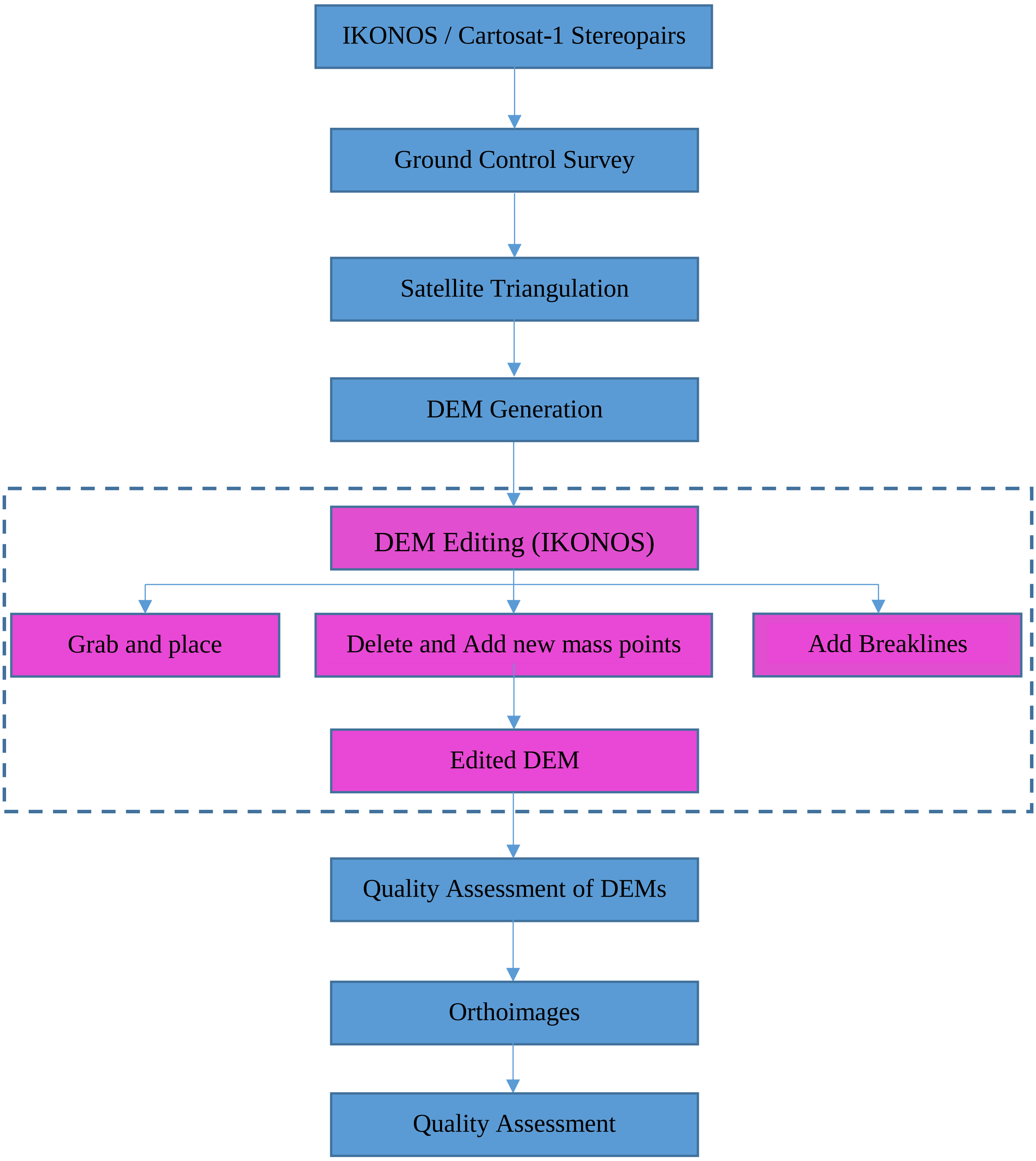

Figure 4. Photogrammetric methodology used for satellite triangulation, DEM and orthoimage generation

The quality assessment of automatically generated DEMs from IKONOS and Cartosat-1 stereopairs is done with respect to the reference DEM generated through manual editing of IKONOS DEM.

4. Results and Discussion

A subset of the DEM generated from Cartosat-1 stereo data (RMSE=0.7) is prepared for the common area with IKONOS DEM. Figure 5, shows the subsets of IKONOS orthoimage, as well as the corresponding DEMs, generated from Cartosat-1 (Carto10 DEM) and IKONOS-2 datasets for the common area. Mass points are shown by blue dots in Figure 6, where a large amount of editing can be observed around the drainage features in the stereo environment of ITE in LPS software. Corrections were done manually to remove erroneous (floating and digging) mass points. Additional mass points and break-lines have been added to represent the terrain correctly. The mass points constituting the triangular irregular network (TIN) depicting the facets on the ground are shown by the vertices of the triangles formed by red coloured lines in Figure 6. The difference image of reference IKONOS DEM and automatically generated IKONOS has a mean difference of 1.421 m. Whereas the difference DEM (dDEM) for the reference IKONOS DEM and Carto10 DEM has a mean difference of 8.74 m [22], [23]. The mean difference between the DSMs of IKONOS and Cartosat-1 is approximately 7.32 m.

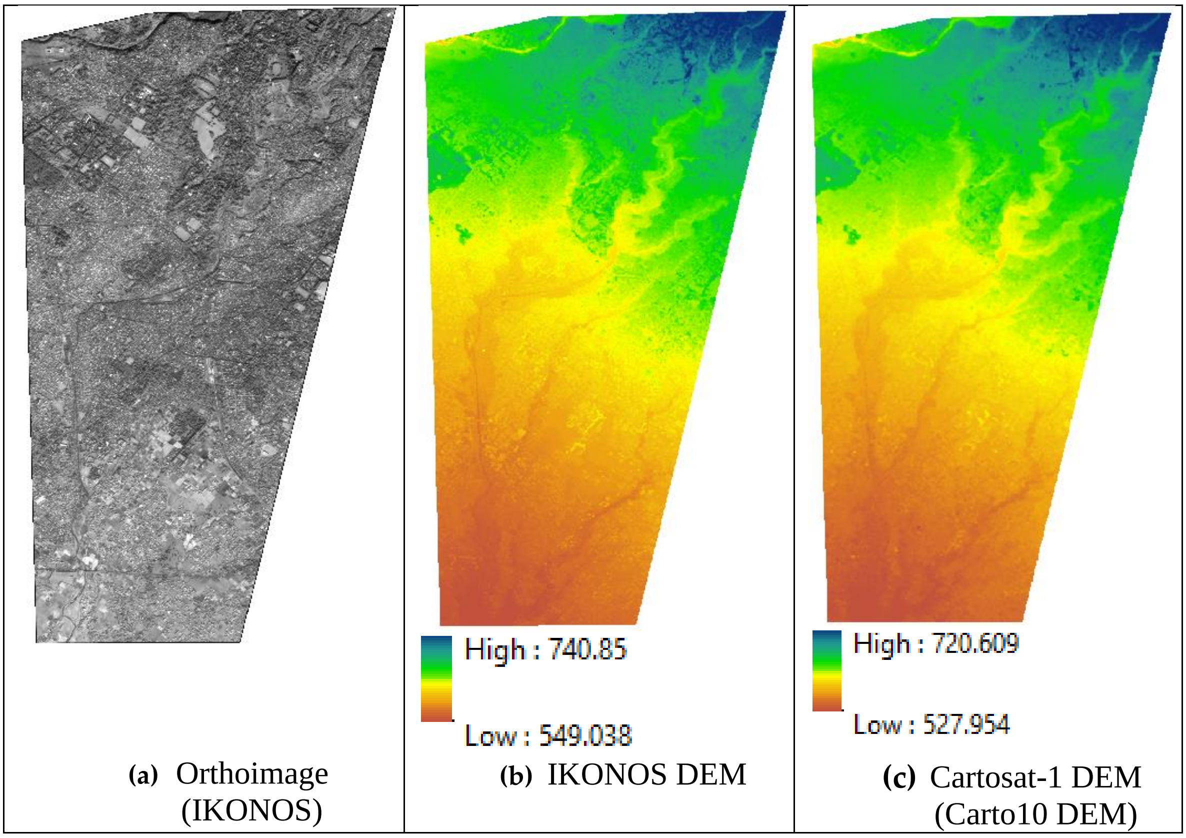

Figure 5. (a) Orthoimage for the reference DEM site, Comparison of (b) reference data (IKONOS DEM) with (c) Cartosat-1 data

The effect of spatial resolution is shown in Figure 7, on optical remote sensing datasets. The features on IKONOS images with 1m spatial resolution (11-bit dynamic range) are much clearly visible than the features on Cartosat-1 data with 2.5 m spatial resolution (10-bit dynamic range). The boundary of the features and thus the transitional boundaries between two features or land use land cover (LULC) classes are more discernible in the VHR dataset i.e., IKONOS images as compared to the HR Cartosat-1 dataset due to both higher spatial resolution as well as the dynamic range of

IKONOS data. The higher spatial resolution, as well as dynamic range of IKONOS data, directly affects the contrast and improved image matching required for conjugate or homologous point selection while computing the parallax difference as part of height measurement. This depicts a clear advantage for VHR data over HR data while photogrammetric processing and generation of resulting products, such as DEM and orthoimage. The quality assessment of the orthoimages shows an improved matching while overlaying of orthoimages generated from the left and the right images due to the removal of ground relief in the DEM editing process and reduced haziness or stretching effects. The accuracies of the DEMs and orthoimages generated from satellite-based stereo datasets can be further improved significantly by the use of more number of well-distributed GCPs [9] strengthening the bundle lock adjustment as part of the satellite triangulation. This can further affect the applications significantly, which are.influenced by the accuracy of the DEM.

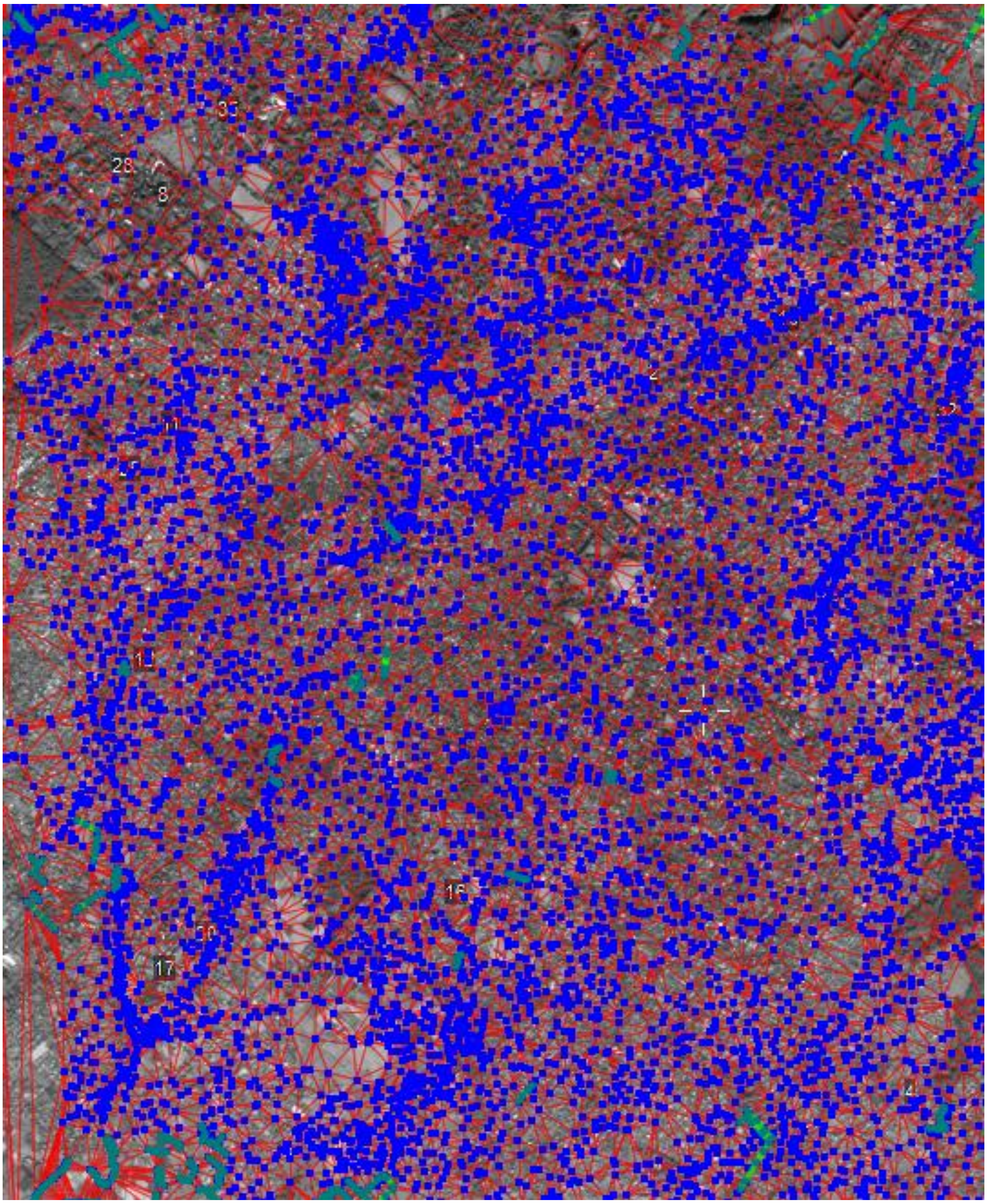

Figure 6. Screenshot of manual editing carried out in Interactive Terrain Editor (ITE, LPS). The mass point, break lines and TIN are visible in the figure on (overlaid) the IKONOS image in stereo.

The study shows that the IKONOS-2 and Cartosat-1 data generate reasonably good DEMs, which can also be assessed using GCPs [9], [24]. However, the quality of automatically generated DEM needs manual editing for improvement due to the presence of the mass points in digging and floating. The mass points present in DEMs are due to the contrast issues in optical data (stereo pair) and requires manual editing for needful corrections. Figure 7 showcases the effect of spatial and spectral resolution in LULC namely, (a) Urban region, (b) road, (c) Urban area across the LULC transition lines. Figure 7 (a) and figure 7 (b) when seen with DSM in ITE shows the mass points transiting from tree canopy to the adjoining urban building areas in hanging (floating state and thus requires manual corrections. Similar hanging and digging mass points are available in regions shown in Figure 7, which were manually corrected for the generation of the reference DEM from IKONOS stereopair.

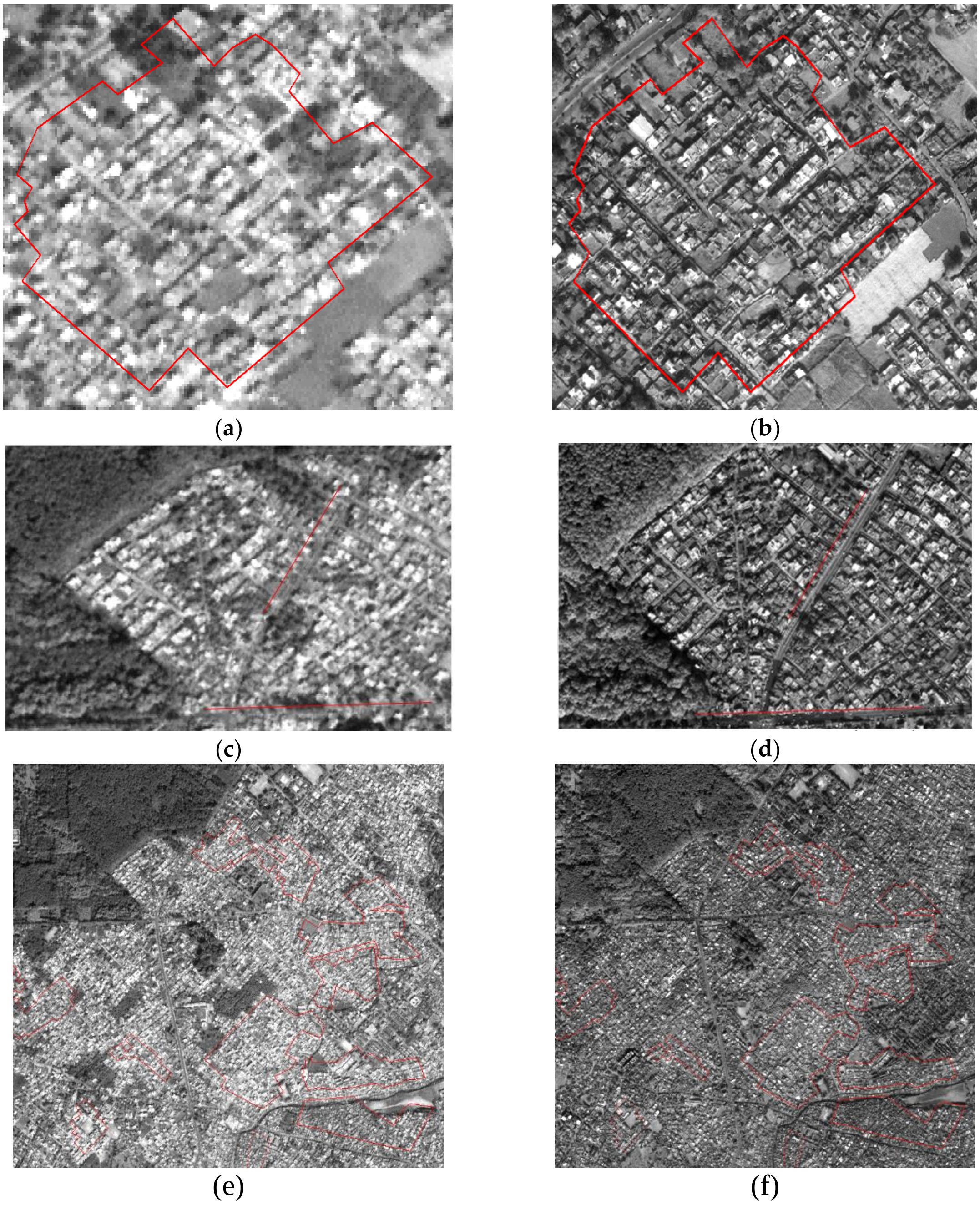

Figure 7. Effect of spatial and spectral resolution (a) Urban region (Cartosat-1), (b) Urban region (IKONOS), (c) road (Cartosat-1), (d) road (IKONOS), (e) Urban area (Cartosat-1), (f) Urban area (IKONOS)

5. Conclusions

The study demonstrates and concludes that the use of edited DEM results in the generation of geometrically improved orthoimage from IKONOS data. It is observed from the 3D visualization of overlaid DEM on stereoview, that the hanging mass points and digging mass points pose challenges in the correction or improvement of DEMs. This can be observed clearly from the visual interpretation of the generated improved orthoimages. Secondly, the edited DEM is used for quantitative assessment of the mean difference in the DEM generated from IKONOS as well as Cartosat-1 stereopair, where the effect of spatial resolution and dynamic range is observed clearly. The study also reveals that the spatial and spectral resolution of IKONOS and Cartosat-1 datasets affect the photogrammetric procedures directly such as GCP marking/pointing, image matching, parallax computation, satellite triangulation, DEMand orthoimage generation.

Acknowledgments: The author would like to thank the space agencies: ISRO, and NASA, along with their collaborators for their insights on benefits as well as applications of satellite-based remote sensing, and effective support to the user community through data-sharing platforms. The authors are highly indebted to Director, IIRS for his continuous support and encouragement for conducting the research activities.

Author Contributions: "A.B., K.J., and R.S.C. conceived and designed the experiments; A.B. performed the experiments; A.B., K.J., and R.S.C. analyzed the data; A.B., K.J., and R.S.C. contributed materials and analysis tools; A.B. wrote the paper."

Conflicts of Interest: The authors declare no conflict of interest.

References

[1] T. M. Lillesand, R. W. Kiefer, and J. W. Chipman, *Remote sensing and image interpretation*. Wiley, 2014.

[2] J. Höhle and M. Potuckova, "Assessment of the quality of digital terrain models," Amsterdam, The Netherlands, 2011.

[3] J. P. Wilson and J. C. Gallant, *Terrain analysis : principles and applications*. Wiley, 2000.

[4] Z. Li, Q. Zhu, and C. Gold, *Digital terrain modeling : principles and methodology*. CRC Press, 2005.

[5] C. P. Sarma, A. Dey, and A. M. Krishna, "Influence of digital elevation models on the simulation of rainfall-induced landslides in the hillslopes of Guwahati, India," *Eng. Geol.*, vol. 268, no. May 2019, 2020.

[6] H. Rahardjo, T. H. Ong, R. B. Rezaur, and E. C. Leong, "Factors controlling instability of homogeneous soil slopes under rainfall," *J. Geotech. Geoenvironmental Eng.*, vol. 133, no. 12, pp. 1532–1543, 2007.

[7] R. Mahalingam and M. J. Olsen, "Evaluation of the influence of source and spatial resolution of DEMs on derivative products used in landslide mapping," *Geomatics, Nat. Hazards Risk*, vol. 7, no. 6, pp. 1835–1855, Nov. 2016.

[8] A. Bhardwaj, R. S. Chatterjee, and K. Jain, "Assimilation of DEMs generated from optical stereo and InSAR pair through data fusion," *Sci. Res.*, vol. 1, no. 3, pp. 39–44, 2013.

[9] A. Bhardwaj, K. Jain, and R. S. Chatterjee, "Generation of high-quality digital elevation models by assimilation of remote sensing-based DEMs," *J. Appl. Remote Sens.*, vol. 13, no. 04, p. 1, Oct. 2019.

[10] R. Deo, C. Rossi, M. Eineder, T. Fritz, and Y. S. Rao, "Framework for Fusion of Ascending and Descending Pass TanDEM-X Raw DEMs," *IEEE J. Sel. Top. Appl. Earth Obs. Remote Sens.*, vol. 8, no. 7, pp. 3347–3355, 2015.

[11] N. Robinson, J. Regetz, and R. P. Guralnick, "EarthEnv-DEM90: A nearly-global, void-free, multi-scale smoothed, 90m digital elevation model from fused ASTER and SRTM data," *ISPRS J. Photogramm. Remote Sens.*, vol. 87, pp. 57–67, Jan. 2014.

[12] D. Yamazaki, D. Ikeshima, J. Sosa, P. D. Bates, G. H. Allen, and T. M. Pavelsky, "MERIT Hydro: A High-

Resolution Global Hydrography Map Based on Latest Topography Dataset," *Water Resour. Res.*, vol. 55, no. 6, pp. 5053–5073, 2019.

[13] H. Papasaika, D. Poli, and E. Baltsavias, "A framework for the fusion of digital elevation models," *Int. Arch. Photogramm. Remote Sens. Spat. Inf. Sci.*, vol. XXXVII, no. Part B2, pp. 811–818, 2008.

[14] D. Yamazaki *et al.*, "A high-accuracy map of global terrain elevations," *Geophys. Res. Lett.*, vol. 44, no. 11, pp. 5844–5853, 2017.

[15] H. D. Betts and R. C. DeRose, "Digital elevation models as a tool for monitoring and measuring gully erosion," *Int. J. Appl. Earth Obs. Geoinf.*, vol. 1, no. 2, pp. 91–101, 1999.

[16] S. Saksena and V. Merwade, "Incorporating the effect of DEM resolution and accuracy for improved flood inundation mapping," *J. Hydrol.*, vol. 530, pp. 180–194, Nov. 2015.

[17] J. P. Leitão and L. M. de Sousa, "Towards the optimal fusion of high-resolution Digital Elevation Models for detailed urban flood assessment," *J. Hydrol.*, vol. 561, pp. 651–661, Jun. 2018.

[18] J. R. Jensen, "Issues involving the creation of digital elevation models and terrain corrected orthoimagery using soft-copy photogrammetry," *Geocarto Int.*, vol. 10, no. 1, pp. 5–21, 1994.

[19] P. S. Roy *et al.*, *Biodiversity Characterization at Landscape Level: National Assessment*. Indian Institute of Remote Sensing, Dehradun, India, 2012.

[20] I. J. Dowman, K. Jacobsen, G. Konecny, and R. Sandau, *High resolution optical satellite imagery*. Whittles Publishing, Caithness, UK, 2012.

[21] K. Jacobsen, "Geometric potential of IKONOS- and QuickBird-images," *Photogramm. Week*, pp. 101–110, 2003.

[22] NRSA Data Center, "CARTOSAT-1 Data User's Handbook," NRSA Data Center, Hyderabad, 2006.

[23] A. Bhardwaj, "Assimilation of Digital Elevation Models Generated from Microwave and Optical Remote Sensing Data," Indian Institute of Technology Roorkee, India, 2018.

[24] A. Bhardwaj, "Assessment of Vertical Accuracy for TanDEM-X 90 m DEMs in Plain, Moderate, and Rugged Terrain," *Proceedings*, vol. 24, no. 1, p. 8, Jun. 2019.